Materials Today: Proceedings 46 (2021) 259–262

Contents lists available at ScienceDirect

Materials Today: Proceedings

journal homepage: www.elsevier.com/locate/matpr

Structure and morphology of yttrium doped barium titanate ceramics for multi-layer capacitor applications

Ravanamma R. [a,b], Muralidhara Reddy K. [b], Venkata Krishnaiah K. [b], Ravi N. [b]

[a] Department of Physics, Jawaharlal Nehru Technological University Anantapur, Anantapuramu, 515002, India
[b] Department of Physics, Rajeev Gandhi Memorial College of Engineering & Technology, Nandyal 518501, India

ARTICLE INFO

Article history:
Received 6 July 2020
Accepted 27 July 2020
Available online 15 September 2020

Keywords:
MLCC
Barium titanate
Y_2O_3
XRD
FTIR
SEM

ABSTRACT

Multilayer ceramic capacitors (MLCCs) are essential components in pulsed power systems (PPS) with high charging and discharging capacity for energy storage applications. Yttrium oxide (Y_2O_3)–doped barium titanate ($BaTiO_3$) (BTY) ceramics with a chemical formula of 60 BaO + (40-x) TiO_2 + x Y_2O_3 (x = 2, 8 and 15) have been synthesized by usual solid state reaction process. These ceramics are analyzed by XRD, FTIR and SEM techniques. The crystalline nature of the undoped $BaTiO_3$ (BT) and Y_2O_3 doped ceramics were confirmed by XRD analysis. In addition, a doublet peak at 30.2° has been shifted to lower angles as the concentration of Y^{3+} ions increases. The functional groups of these BT and BTY2 ceramics were investigated using FTIR analysis. Morphological studies were performed through scanning electron microscopy (SEM), revealing the average particle size of BT 331 nm and BTY2 136 nm from Image-J software.

Selection and peer-review under responsibility of the scientific committee of the 2nd International Conference on Manufacturing Material Science and Engineering.

1. Introduction

In these modern years, especially in pulsed power systems (PPS), dielectric capacitors have been widely developed due to their high energy density and extremely fast charging and discharging. High performance capacitors with high energy density, good thermal capacity stability and high charge efficiency have been reduced the volume and weight of PPS [1]. Multilayer ceramic capacitors (MLCC) have been effectively used to increase the volumetric efficiency of capacitive components [2]. With dielectric layers of small thicknesses arranged in parallel, higher capacitance levels can be achieved along with miniaturization of the electronic circuitry. The electronic devices, which we are using every day, such as smartphones, computers and LED TVs contain more than 1000 of MLCCs. For electric vehicles, more than 10,000 MLCCs are needed due to their electronic control and automation system [3]. Barium titanate ($BaTiO_3$) with a perovskite structure is suitable for MLCC applications due to (BT) high-dielectric constant. Moreover, It can be used as a capacitor with small in size and high-capacitance due to large relative permittivity of 1,000 to 20,000. The $BaTiO_3$ MLCC have been found in the electronics industry for transducers, actuators and high dielectrics applications [4].

Rare earth (RE^{3+}) ions such as Dy^{3+}, Ho^{3+}, Sm^{3+}, La^{3+}, Yb^{3+}, or Y^{3+} have been envisioned to replace Ba and Ti cations in the $BaTiO_3$ structure, but Dy^{3+}, Ho^{3+}, and Y^{3+} also unveil amphoteric behavior and pronounced as being supportive in extending the lifetime of the MLCCs [5]. Y_2O_3 is generally considered as a dopant in the commercial formulation of powders for the fabrication of MLCCs at an industrial scale. Moreover, it results in similar properties compared to adding other RE^{3+} ions.

This present work aims to discuss the structural and morphological studies of Y_2O_3 doped $BaTiO_3$ ceramics for MLCC applications. In the stoichiometric ratio, the powders were prepared by conventional solid state method. The calcined and sintered fine powder samples were investigated through XRD, FTIR and SEM analyses.

2. Experimental

The following raw materials were used to prepare the Y_2O_3 doped $BaTiO_3$ powders: Barium carbonate ($BaCO_3$) with 99%, and titanium dioxide (TiO_2) with 99.9% and Y_2O_3 (99.99%, Aldrich). A batch of 15 g of Y_2O_3 doped $BaTiO_3$ powder was prepared using the composition 60 BaO + (40-x) TiO_2 + x Y_2O_3 (BTY) (where x = 2,

E-mail addresses: kvkphd84@gmail.com (K. Venkata Krishnaiah), ravi2728@gmail.com (N. Ravi)

https://doi.org/10.1016/j.matpr.2020.07.646
2214-7853/
Selection and peer-review under responsibility of the scientific committee of the 2nd International Conference on Manufacturing Material Science and Engineering.

8 and 15) by solid state reaction method. The mixture was heated at 400 °C for 1 h to eliminate carbonates (CO_2) and other hydroxyl groups. Later the composition was ground for 12 h with the help of agate mortar and pestle under ethanol as a medium. Powder was calcined using electrical furnace at 1000 °C for 8 h with heating and cooling rate of 4 °C/min and then it is allowed to cool to room temperature. The paraffin of 0.5 wt% was added to the powder mixture as a binder medium at room temperature. The cylindrical discs were prepared by a hydraulic pressure of 10 MPa using steel dies with a thickness of 2.3 mm and diameter of 11.5 mm. These pellets are annealed again at 400 °C for 1 h to eliminate the binder from the samples. Then the pellets were sintered at 1200 °C for 6 h with a heating rate of 4 °C/min. The powder samples are used for further studies.

Bruker Optik GmbH IR spectrometer was used to record IR spectra from 500 to 3000 cm^{-1}. RIGAKU X-ray diffractometer (Miniflex-600) with $CuK_{\alpha 1}$ radiation source with wavelength 1.54059 A° (power: 35 V × 15 mA) was utilized to record diffraction pattern of the powder. Scanning electron microscope (SEM) images were captured using JEOL JSM-IT 500 series.

3. XRD analysis

XRD profile of undoped BT sample is shown in Fig. 1(a). From the XRD analysis, undoped BT sample exhibit a tetragonal structure which infers that a doublet peak in the range of 44 – 45° with corresponding indices (002) and (200). On the other hand, above T_c, the cubic phase provides only a single peak in the same region with (200) indices. However, $BaTiO_3$ particles below T_c were unveiled tetragonal phase owing to existence of a doublet in the region of (44–45°) [6].

XRD pattern of Y_2O_3 (2, 8, 15 mol%) doped BTY ceramics are shown in Fig. 1(b). A doublet intense peak at 30.2° is noticed which shifts towards lower angle side in the BTY samples as the Y^{3+} ion concentration increases with 2, 8 and 15 mol%. Peak positions of the BT and BTY samples are represented in the Table 1. The intensity of the doublet decreases with increase of Y^{3+} ion concentration at 30.2° and appears as a single peak at higher concentration which is clearly seen in the inset of Fig. 1(b). On the other hand, full width at half maximum (FWHM) for 2 mol% of Y_2O_3 is 1.669 and then decreases with increase of Y_2O_3 concentration. Except the peak at 42° in 15 mol% of Y_2O_3, all peaks in the XRD spectra of the concentrations are unveiled as a single peak because of its cubic phase. Most peaks in the BTY2 sample, with the exception of a few peaks at 24° and 30°, show differences in relative density, which can be attributed to structural deformation due to the addition of impurities, Y^{3+} ions [7]. This effect is mainly due to the difference in ionic radii between the main component (BT) and the doping (Y^{3+}) ions. FWHM drops to 0.518, so crystal volume decreases with increasing dopant concentration.

Table 1
Peak position, FWHM of the samples from XRD measurements.

Sample Name	Peak position	FWHM of peak
BT	24.22	0.216
BTY2	30.2	1.669
BTY8	29.44	0.985
BTY15	29.48	0.518

4. FTIR spectra

FTIR spectra of undoped BT and Y_2O_3-doped $BaTiO_3$ powders were recorded at room temperature in the wavenumber range of 400–4000 cm^{-1}, as shown in the Fig. 2. The IR bands were resolved at 694 cm^{-1}, 681 cm^{-1}, 854 cm^{-1}, 856 cm^{-1}1, 1064 cm^{-1}, 1444 cm^{-1}, 1432 cm^{-1}, 1749 cm^{-1}, 2340 cm^{-1}, 2455 cm^{-1} and 2821 cm^{-1} for both BT and BTY. It is clear that there is no further molecular fingerprint of free $BaCO_3$ below 600 cm^{-1}. All the samples have a characteristic vibration of Ti-O-Ti and Ti-O bonds between 600 cm^{-1} and 800 cm^{-1} which is owing to molecular vibrations of $BaTiO_3$ [8]. As a result, a band is obtained at 694 cm^{-1} for BT, whereas band at 681 cm^{-1} for BTY samples correspond to the vibrations of Ti-O-Ti and Ti-O-Y bonds, respectively [9]. The band at 694 cm^{-1} shifts towards lower energy side owing to Y^{3+} ions in the BT. Band at 854 cm^{-1} is araised in both BT and BTY samples that attributes to Ti-O vibration. A strong absorption band is positioned at 1444 cm^{-1} and 1432 cm^{-1} for BT and BTY samples due to Ba/Y-Ti-O bonds. A peak at 1749 cm^{-1} is due to symmetric bond of Ba-O for BT and Ba/Y-O for BTY. Bands at 2455 cm^{-1} and 2821 cm^{-1} are attributed to H_2O and O–H stretching bonds [10]. No significant effect of H_2O and OH^- were noticed on BT and BTY owing to high preparation temperature of the samples.

5. SEM analysis

The morphology of these ceramics was analyzed by scanning electron microscope (SEM) on the BT and BTY samples. SEM images of undoped BT and Y_2O_3 doped BTY2 ceramics are presented in various resolutions displayed in the Fig. 3. As perceived in

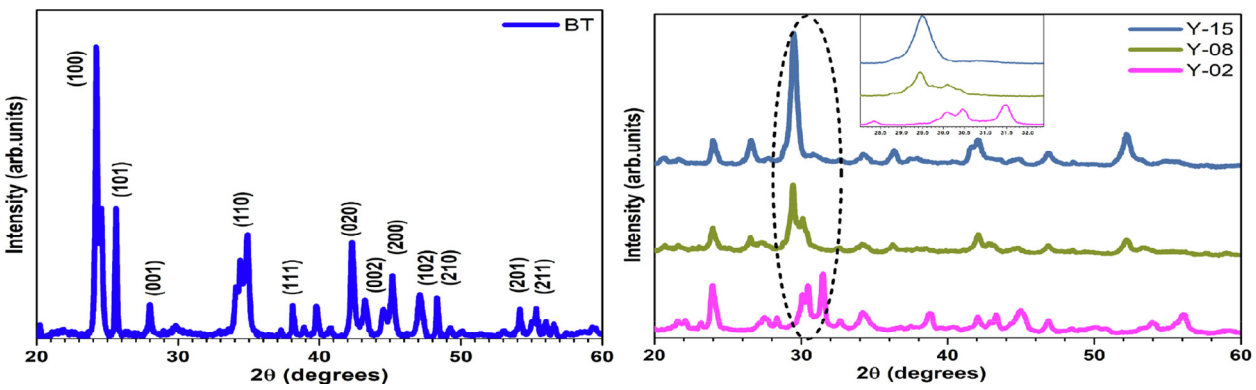

Fig. 1. (a) & (b). XRD profiles of undoped BaTiO and Y_2O_3 doped $BaTiO_3$.

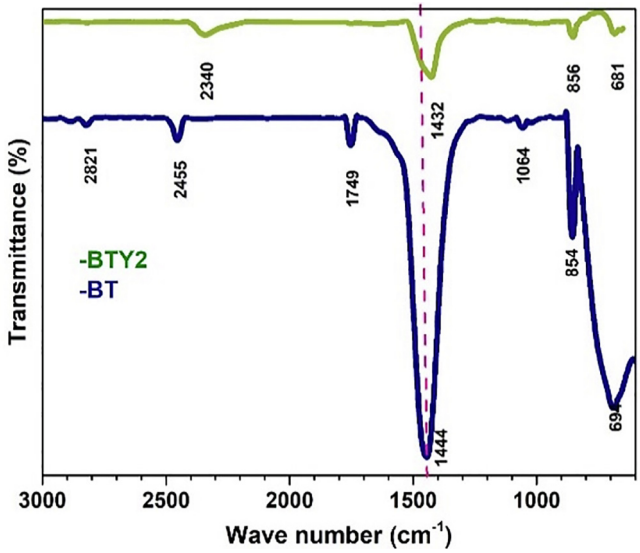

Fig. 2. FTIR spectra of undoped BaTiO and 2 mol% of Y_2O_3 doped $BaTiO_3$.

Fig. 3(a), undoped BT illustrate a very dense microstructure with a grain size of 331 nm. Fig. 3(b) demonstrate the microstructures of Y_2O_3-doped BTY2 with a grain size of 136 nm. Compared to BT sample, the grain size of BTY2 sample is much smaller. These results are correlated with the results obtained by XRD. As we known that the grain growth of ceramics depends primarily on the diffusion during the sintering. The development of the oxygen vacancies induced by Y^{3+} acceptor-doping and their motion are accelerating the diffusion and reduce the grain size in BTY2 [11]. Further, the grain size decreases with increase in Y_2O_3 concentration. From SEM images, it is worthy to mention that the nanosized BTY particles are formed even with the solid-state synthesis, but they are utterly agglomerated. However, when heat treatment is performed on Y_2O_3 -doped BTY2 samples, they are obtained uniform nanosized particles, as shown in Fig. 3b. Compared to undoped $BaTiO_3$, Y_2O_3 -doped $BaTiO_3$ is revealed with nanosized particles which is suitable for energy storage applications. Further studies under way to realize these Y_2O_3-doped $BaTiO_3$ for MLCCs applications. The average gran size of BT and BTY2 were evaluated using IMAGE-J software.

6. Conclusion

Y_2O_3–doped $BaTiO_3$ (BTY) and undoped $BaTiO_3$ (BT) ceramics have been prepared by solid state reaction method for high energy storage applications. The XRD has been confirmed crystalline nature of BT and BTY with a tetragonal structure. With the increase of doping concentration of Y_2O_3, the tetragonal structure has been transformed to cubic structure due to increase of the Y^{3+} ions in BTY samples. A small shift to the lower energy has been observed in the BTY2 sample compared to BT in FTIR spectra. SEM images have been confirmed the size of the crystallites in the nano range with fine microstructures.

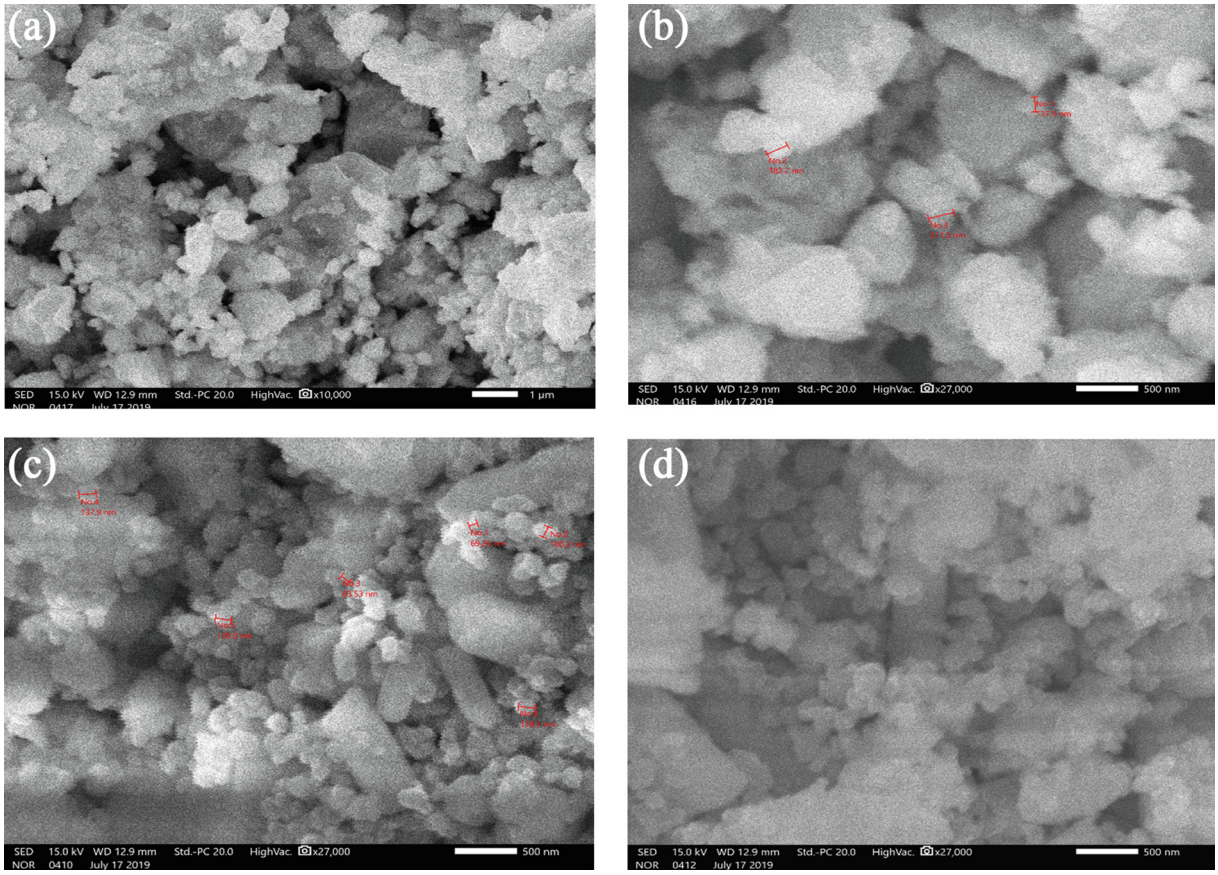

Fig. 3. (a) & (b). SEM images of undoped $BaTiO_3$ powder (c) & (d). SEM images of 2 mol% of Y_2O_3 doped $BaTiO_3$ powder.

CRediT authorship contribution statement

R. Ravanamma: Investigation, Methodology. **K. Muralidhara Reddy:** Supervision. **K. Venkata Krishnaiah:** Conceptualization, Formal analysis. **N. Ravi:** Writing - original draft, Writing - review & editing.

Declaration of Competing Interest

The authors declare that they have no known competing financial interests or personal relationships that could have appeared to influence the work reported in this paper.

References

[1] W. Li, D.i. Zhou, X.u. Ran, D.-W. Wang, S.u. Jinzhan, L.-X. Pang, W. Liu, G.-H. Chen, BaTiO3-Based Multilayers with Outstanding Energy Storage Performance for High Temperature Capacitor Applications, ACS Appl. Energy Mater. 2 (8) (2019) 5499–5506.

[2] N. Kumar, A. Ionin, T. Ansell, S. Kwon, W. Hackenberger, D. Cann, Multilayer ceramic capacitors based on relaxor $BaTiO_3$-$Bi(Zn_{1/2}Ti_{1/2})O_3$ for temperature stable and high energy density capacitor applications, Appl. Phys. Lett. 106 (2015) 252901.

[3] K. Hong, Tae Hyung Lee, Jun Min Suh, Seok-Hyun Yoon and Ho Won Jang, Perspective and challenges in multilayer ceramic capacitors for next generation electronics, J. Mater. Chem. C 7 (2019) 9782–9802.

[4] J. Chen, Z. Feng, X7R dielectric multilayer ceramic capacitors show good micro-actuating properties with little hysteresis, Electronics Letters 50 (7) (2014) 538–540.

[5] Ana María Hernández-López, Juan Antonio Aguilar-Garib, Sophie Guillemet-Fritsch, Roman Nava-Quintero, Pascal Dufour, Christophe Tenailleau, Bernard Durand and Zarel Valdez-N, Reliability of X7R Multilayer Ceramic Capacitors During High Accelerated Life Testing (HALT) Materials (2018), 11, 1900.

[6] Z.M. Tsikriteas, G.C. Manika, A.C. Patsidis, G.C. Psarras, Probing the multifunctional behaviour of barium zirconate/barium titanate/epoxy resin hybrid nanodielectrics, J Therm Anal Calorim (2020), https://doi.org/10.1007/s10973-020-09855-w.

[7] G. Bhavania, S. Ganesanb, Structural, Morphological and Optical Study of Bismuth and Zinc Co-Doped Yttrium Oxide Prepared by Solvothermal and Wet Chemical Method, Acta Physica Polonica A 130 (6) (2016) 1373–1379.

[8] X.N. Zhu, W. Zhang, X. Chen, Enhanced dielectric and ferroelectric characteristics in Ca-modified BaTiO3 ceramics AIP Adv. 3 2013 2646.

[9] Q. Xu, M.T. Lanagan, W. Luo, Electrical properties and relaxation behavior of$Bi_{0.5}Na_{0.5}TiO_3$-$BaTiO_3$, ceramics modified with $NaNbO_3$, J. Eur. Ceram. Soc. 36 (2016) 2469–2477.

[10] D. Morrison, D.C. Sinclair, A.R. West, Characterization of lanthanum doped barium titanate ceramics using impedance spectroscopy, J. Am. Ceram. Soc. 84 (3) (2001) 531–538.

[11] M. Khajelakzay, Reza Shoja Razavi, Masoud Barekat, and Mahdi Naderi, Synthesis of Yttria Nanopowders by Two Precipitation Methods and Investigation of Synthesis Conditions, Int. J. Appl. Ceram. Technol. 13 (1) (2016) 209–218.